

Published in final edited form as:

*Invest Ophthalmol Vis Sci.* 2006 May ; 47(5): 2114–2124. doi:10.1167/iovs.05-1068.

## Mitochondrial Potassium ATP Channels and Retinal Ischemic Preconditioning

Steven Roth<sup>1,2,3</sup>, John C. Dreixler<sup>1</sup>, Afzhal R. Shaikh<sup>1</sup>, Katherine H. Lee<sup>1</sup>, and Vytautas Bindokas<sup>2</sup>

<sup>1</sup>From the Department of Anesthesia and Critical Care, the University of Chicago, Chicago, Illinois.

<sup>2</sup>Department of Neurobiology, the University of Chicago, Chicago, Illinois.

<sup>3</sup>Department of Molecular Medicine, the University of Chicago, Chicago, Illinois.

### Abstract

**PURPOSE**—To examine the mechanisms of ischemic preconditioning (IPC) related to the opening of mitochondrial KATP (mKATP) channels in the retina.

**METHODS**—Rats were subjected to retinal ischemia after IPC, or retinas were rendered ischemic after pharmacological opening of mKATP channels. The effects of blocking mKATP channel opening, nitric oxide synthase (NOS) subtypes, or protein kinase C (PKC) on the protective effect of IPC or on the opening of mKATP channels were studied. Electroretinography assessed functional recovery after ischemia. Immunohisto-chemistry and image analysis were used to measure changes in levels of reactive oxygen species (ROS) and NOS subtypes and to determine their cellular localization.

**RESULTS**—IPC was effectively mimicked by injection of the mKATP channel opener diazoxide. Both IPC and its mimicking by diazoxide were completely attenuated by the mKATP channel blocker 5-hydroxydecanoic acid (5-HD). Nonspecific blockade of NOS by *N*<sub>ω</sub>-nitro-L-arginine (L-NNA), but not by specific inducible (i)NOS or neuronal (n)NOS inhibitors, blunted IPC and IPC-mimicking, as did blockade of PKC. IPC and diazoxide IPC-mimicking significantly enhanced mitochondrial ROS production in the inner retina, an effect blocked by 5-HD. Mitochondrial ROS colocalized with e- and nNOS in retinal cells after stimulation with diazoxide.

**CONCLUSIONS**—The results showed that IPC in the retina requires opening of the mKATP channel, and that IPC could be effectively mimicked using the mKATP channel opener diazoxide. eNOS-generated nitric oxide, PKC, and ROS are activated by opening of the mKATP channel.

Novel functions including protection against ischemia have been assigned to ion channels of the inner mitochondrial membrane (i.e., the mitochondrial KATP channel; mKATP). The mKATP channel, which has not yet been cloned, is composed of sulfonylurea receptor-like (SUR) and inward rectifier-like (Kir) components smaller than their surface membrane counterparts.<sup>1</sup> Brain mitochondria predominantly contain Kir6.1 and a SUR2-related subunit, approximately seven times the quantity present in myocardium.<sup>2</sup> Mitochondrial channels are thought to be the main KATP effector of ischemic preconditioning (IPC) in myocardium and the principal KATP channel in the brain.<sup>3</sup>

Corresponding author: Steven Roth, Department of Anesthesia and Critical Care, University of Chicago, 5841 South Maryland, Box MC-4028, Chicago, IL 60637; sroth@dacc.uchicago.edu..

Disclosure: **S. Roth**, None; **J.C. Dreixler**, None; **A.R. Shaikh**, None; **K.H. Lee**, None; **V. Bindokas**, None

The publication costs of this article were defrayed in part by page charge payment. This article must therefore be marked “advertisement” in accordance with 18 U.S.C. §1734 solely to indicate this fact.

In opposition to mitochondrial dysfunction causing neuronal injury, opening of the mKATP channel protects cerebral cortical cells against damage from hypoxia *in vitro* and *in vivo* and is essential for chemical preconditioning *in vitro*.<sup>4-9</sup> Retinal cell cultures exposed to glutamate were protected by the mKATP channel opener diazoxide.<sup>10</sup> The mechanisms whereby mKATP channel opening protect have not been completely defined, but may include upregulation of neuroprotective or antiapoptotic genes, as well as enhanced preservation of ATP.<sup>11,12</sup>

In previous studies, we demonstrated robust amelioration of retinal ischemic injury by prior IPC.<sup>13</sup> Earlier studies from our laboratory and confirmed by others have indicated the essential role of adenosine, protein kinase C (PKC), the opening of KATP channels, and decreased retinal cell apoptosis in this neuroprotection.<sup>14-16</sup> In the present study, we examined the hypothesis that the mKATP channel is an effector of IPC-induced neuroprotection. The mechanisms whereby mKATP channel opening is protective were studied by examining the roles of postulated downstream mediators including PKC, nitric oxide (NO), and reactive oxygen species (ROS). Our results indicate the presence of intrinsic neuroprotective signaling in the retina involving mKATP, PKC, NO, and ROS.

## MATERIALS AND METHODS

### Ischemia Methodology

Procedures<sup>13,17</sup> conformed to the ARVO Statement for the Use of Animals in Ophthalmic and Vision Research and were approved by our Animal Care Committee. Sprague-Dawley rats (200 -250 g) purchased from Harlan (Indianapolis, IN) were maintained on a 12-hour on—off light cycle, and were dark adapted for at least 2 hours before experiments. Before ischemia was induced, animals were anesthetized with choral hydrate, 450 mg/kg intraperitoneally (IP). For baseline and postischemia follow-up electroretinograms, rats were injected IP with ketamine (Parke-Davis, Morris Plains, NJ) 35 mg/kg, and xylazine (Miles, Shawnee Mission, KS) 5 mg/kg. Corneal analgesia was achieved using 1 to 2 drops of 0.5% proparacaine (Allergan, Humacao, Puerto Rico). Pupillary dilatation was maintained with 0.5% tropicamide (Alcon, Humacao, Puerto Rico) and cyclopentolate HCl 0.2% and 1% phenylephrine HCl (Cyclomydril; Alcon, Fort Worth, TX). Body temperature was maintained at 36.5 to 37.0°C with a servocontrolled heating blanket (Harvard Apparatus, Natick, MA).

For preconditioning, the intraocular pressure (IOP) was increased to 160 mm Hg for 8 minutes using a pressurized 1000-mL plastic container of sterile normal saline (Baxter, North Chicago, IL), connected to a 27-gauge needle placed in the anterior chamber of the eye. For ischemia, the IOP was increased to 110 mm Hg by elevating the saline reservoir above the eye for 45 minutes.<sup>17,18</sup> The degree of IOP elevation differed for IPC and ischemia because in our previous studies,<sup>18</sup> we found that IPC protection was more consistently produced using a higher pressure for the required brief ischemic stimulus. In sham, nonpreconditioned animals, the IOP was maintained at 10 to 15 mm Hg. The opposite eye of each animal served as a nonischemic control.

### Electroretinography

Procedures used in our laboratory have been described in detail previously.<sup>19,20</sup> In brief, responses to 10- $\mu$ s white light flashes on a Ganzfeld (Nicolet; Madison, WI) were recorded (Spirit 486 System; Nicolet). Data are the average of three flashes delivered at least 2 minutes apart. The ERG wave amplitudes 7 days after ischemia were measured and reported as a percentage of the baseline, nonischemic wave amplitude.

## Immunohistochemistry

Enucleated eyes were fixed at room temperature in 4% paraformaldehyde for 3 hours. After removal of the anterior segment, the posterior portion of the eye was postfixed in the same fixative overnight at 4°C before being placed in 25% sucrose for a second overnight period at 4°C for cryoprotection. Eye cups were embedded in optimal cutting temperature (OCT) compound (Sakura Finetec, Torrance, CA) and were cut into 10- $\mu$ m-thick cryosections.<sup>17,21</sup>

Primary antibodies (all at 1:50 concentration) included mouse monoclonal anti-eNOS/NOS3 (BD PharMingen, San Diego, CA), rabbit polyclonal anti-iNOS/NOS2 (Santa Cruz Biotechnology, Santa Cruz, CA), rabbit polyclonal anti-nNOS/brain NOS (Sigma-Aldrich, St. Louis, MO), biotin-conjugated mouse monoclonal anti-Thy-1 (BD PharMingen), Alexa Fluor 488-conjugated mouse anti-OxPhos Complex IV subunit I (Invitrogen, Carlsbad, CA), rabbit polyclonal anti-OX42 (BD PharMingen), rabbit polyclonal anti-caveolin-1 (Santa Cruz Biotechnology), and mouse monoclonal anti-glial fibrillary acidic protein (GFAP; Sigma-Aldrich). Nuclei were identified with a green nucleic acid stain (slide incubated 5 minutes with Sytox 1:500; Invitrogen), or with 4',6'-diamino-2-phenylindole (DAPI; Oncogene Research, San Diego, CA). Sections were then exposed to the appropriate secondary antibodies: fluorescein-conjugated avidin, (1:500, Jackson ImmunoResearch, West Grove, PA), goat anti-mouse IgG FITC-conjugate (1:500; Southern Biotechnology, Birmingham, AL), goat anti-rabbit IgG cascade blue conjugate (1:500; Invitrogen), or goat anti-rabbit IgG fluorescein conjugate (1:500, Invitrogen). Antifade mounting medium (Dako, Carpinteria, CA) was applied and sections were coverslipped.

## Imaging

We used a fluorescence microscope (inverted microscope model IX81; Olympus, Lake Success, NY), a chilled charge-coupled device (CCD) camera (Retiga Fast firewire EXi; QImaging, Burnaby, BC, Canada), and a 60x oil lens. Excitation/dichroic/emission settings were 480/40 nm-505LP-535/30 nm (MitoTracker; Invitrogen) and 530 to 550 nm -570DM-590LP for greens (FITC and fluorescein).

## Fluorescent Labeling of ROS

To investigate the origin of ROS, we injected 2  $\mu$ L of a red fluorescent dye (reduced MitoTracker Red; CM-H<sub>2</sub> XROS 100  $\mu$ M [Invitrogen] and 1% dimethyl sulfoxide [DMSO] in phosphate buffered-saline [PBS]) into the vitreous, or 5 mg/kg dihydroethidium (HET; Invitrogen) IP in 5% DMSO in PBS, 15 minutes before IPC (160 mm Hg pressure for 8 minutes), or diazoxide (40 mg/kg), or DMSO vehicle control. The eyes were removed 15 minutes or 1, 6, or 24 hours later.

## Image Analysis

Quantification of the fluorescence intensities was performed using NIH ImageJ v.1.33 (available by ftp at [zippy.nimh.nih.gov/](http://zippy.nimh.nih.gov/) or at <http://rsb.info.nih.gov/nih-image/>; developed by Wayne Rasband, National Institutes of Health, Bethesda, MD), adapted from our previous methods.<sup>17</sup> The mean intensity was determined in five equal-sized regions, extending from the retinal ganglion cell layer to the inner nuclear layer. The regions were approximately evenly spaced in the viewed image. The mean intensities were normalized to the paired normal eye for the IPC experiments and to the fluorescence exposure levels at the 15-minute time point for the diazoxide/DMSO experimentation.

## Studies

To examine the role of mKATP channels in retinal IPC, a dose-response study was performed using the specific mKATP antagonist 5-hydroxydecanoic acid (5-HD; 1, 10, and 40 mg/kg;

Sigma-Aldrich), injected 15 minutes before IPC, followed by 45 minutes of ischemia 24 hours later. To examine whether the opening of mKATP channels could mimic IPC, we injected the mKATP channel opener diazoxide (Sigma-Aldrich) 5, 10, or 40 mg/kg 30 minutes or 24 hours before 45 minutes of ischemia. Having determined optimal dosage and timing to mimic IPC with diazoxide, we examined the mechanisms of neuroprotection by opening of mKATP channels. To examine the role of PKC, we injected the PKC antagonists bisindolylmaleimide-1 15  $\mu$ M or 1.5 mM (Bis1; Calbiochem, San Diego, CA), 250 nM, chelerythrine chloride 25  $\mu$ M or 2.5 mM (Sigma-Aldrich), or PBS vehicle into the vitreous of both eyes 15 minutes before diazoxide. To test the involvement of NO, we injected *N*<sub>ω</sub>-nitro-L-arginine (L-NNA; Sigma-Aldrich) 30 mg/kg as a nonspecific antagonist of NOS, 1400W (Tocris, Ellisville, MO; 20 or 50 mg/kg) to block iNOS specifically, and 7-nitroindazole (7-NI, 50 and 100 mg/kg; Sigma-Aldrich) to block nNOS specifically, 1 hour before injection of diazoxide or IPC. The outcome after ischemia was assessed using electroretinography. Levels of eNOS, iNOS, and nNOS were quantitated using immunohistochemistry and image analysis.

To evaluate the role of ROS in IPC or diazoxide-induced IPC mimicking, rats were injected intravitreally with a mitochondrial ROS marker (reduced MitoTracker Red; Invitrogen). Retinal sections were examined 15 minutes to 24 hours after IPC or diazoxide injection. Another ROS indicator, HET, was used to confirm and support the findings with the fluorescent tracer. Immunohistochemistry and double or triple labeling were used to localize ROS in the retina.

Data (expressed as the mean  $\pm$  SEM) were analyzed as previously described, with ANOVA and post hoc *t*-tests (Stata ver. 6.0; Stata, College Station, TX). Results between paired eyes were compared by paired *t*-test and between time-matched groups from different animals by unpaired *t*-test. *P* < 0.05 denoted statistical significance.<sup>19,20</sup>

## RESULTS

### Effect of mKATP Channel Opening Recovery after Ischemia

IPC resulted in b-wave recovery after ischemia of 90%  $\pm$  6% relative to baseline, comparable to that in our previous studies.<sup>17,21</sup> 5-HD significantly blunted this protective effect at 1 mg/kg (56%  $\pm$  10%; *P* < 0.03) and 40 mg/kg (36  $\pm$  4, *P* < 0.005), but the effect at 10 mg/kg (74%  $\pm$  8%) was not significant (Fig. 1). Opening the mKATP channel by systemic administration of diazoxide 24 hours before ischemia resulted in a significant dose-dependent improvement in recovery (Fig. 2). At the highest dose, 40 mg/kg, recovery was 64%  $\pm$  6% (*P* < 0.004 compared with DMSO-based vehicle, 30%  $\pm$  8%). This protective effect of diazoxide was completely antagonized by 5-HD injection (27%  $\pm$  4%; *P* < 0.0003 vs. diazoxide without 5-HD; Fig. 2), comparable to the result with DMSO vehicle and ischemia (30%  $\pm$  8%). There was no improvement in recovery if diazoxide was injected 30 minutes before ischemia (data not shown). Neither 5-HD nor diazoxide had any significant effect on the nonischemic eye. In a group of four rats, we monitored the arterial blood pressure from a cannulated iliac artery for 2 hours after injection of diazoxide 40 mg/kg. The average decrease in mean arterial blood pressure was 10%.

### Localization of Nitric Oxide and PKC in Relation to mKATP Channels

The NOS inhibitor L-NNA, 30 mg/kg IP 2 hours before IPC, completely attenuated IPC's protective effect (Fig. 3). Recovery after IPC + L-NNA and ischemia was 38%  $\pm$  8% (*P* < 0.01 vs. 90%  $\pm$  6% for IPC without L-NNA + ischemia), compared to 33%  $\pm$  4% for ischemia without prior IPC (sham IPC). The IPC-mimicking effect of diazoxide was blocked by L-NNA 30 mg/kg IP (33%  $\pm$  4%, *P* < 0.002); by injection into the vitreous 15 minutes before diazoxide of the PKC inhibitor (Fig. 4) Bis1<sup>22</sup> 15  $\mu$ M (25%  $\pm$  7%, *P* < 0.009) and 1.5 mM (33%  $\pm$  4%,

$P < 0.008$ ); and by chelerythrine chloride<sup>23</sup> 250 nM ( $27\% \pm 8\%$ ,  $P < 0.01$ ), 25  $\mu\text{M}$  ( $7\% \pm 5\%$ ,  $P < 0.0001$ ), and 2.5 mM ( $9\% \pm 3\%$ ,  $P < 0.0001$ ). Despite the blockade of diazoxide IPC-mimicking by L-NNA, there was no effect of the specific nNOS inhibitor 7-NI (50 and 100 mg/kg) or the iNOS inhibitor 1400W (20 and 50 mg/kg; Fig. 5).

### Expression of NOS Isoforms

After IPC, or IPC-mimicking by diazoxide, there were significant increases in immunostaining for e-, i-, and nNOS from 15 minutes to 24 hours (Figs. 6, 7). The patterns of increased eand nNOS were similar, but differed for iNOS. Whereas iNOS increased at 15 minutes, 1 hour, and 6 hours after IPC, it increased only at 15 minutes after diazoxide. The increases in NOS subtypes after IPC and diazoxide were primarily in the retinal ganglion cell (RGC) and inner plexiform layer (IPL). Increased NOS subtypes (Figs. 8, 9) were blunted by 5-HD. Note that different imaging exposure times were used for Figures 8 and 9 than for Figures 6 and 7, and thus images should not be directly compared. Normalization was performed in all cases, as stated in the Methods section.

### ROS after IPC and Diazoxide

Initially, to test the feasibility of measuring ROS and to confirm that we were detecting mitochondrial ROS, we used a positive control of 45 minutes of ischemia followed by 1 hour of reperfusion. ROS were measured in retinal cryosections using a red fluorescent label (reduced MitoTracker Red; Invitrogen; Fig. 10). Confirmation of the method was provided using the alternate ROS indicator, HET (Fig. 11). Both Figures 10 and 11 show that little positive staining was apparent in the nonischemic negative control retinal section. Double-labeling with antibodies to the inner mitochondrial membrane protein cytochrome oxidase IV subunit (COX IV) confirmed mitochondrial ROS localization of both the red fluorescent label and HET. Double-labeling with thy-1 and the green nucleic acid stain (Sytox; Invitrogen) showed ROS in RGCs and in the IPL. Only weak staining for ROS was evident in cells stained for glial fibrillary acidic protein (GFAP).

Fig. 12 shows triple labeling for COX IV, the red fluorescent dye (MitoTracker Red; Invitrogen), and DAPI-stained nuclei in retinas studied 1 hour after diazoxide injection (as do the succeeding Figs. 13 and 14). COX IV and red fluorescence colocalization may be seen in the RGCs, nerve fiber, and IPL. The tracer colocalized in retinal cells with eNOS and nNOS, but not with iNOS (Fig. 13). On triple labeling (Fig. 13), eNOS colocalized with the red fluorescent marker and the endothelial cell endogenous eNOS inhibitor caveolin-1; nNOS and red fluorescence were found in RGCs and displaced amacrine cells by labeling cell nuclei with DAPI; iNOS was identified in microglia by double-labeling with OX42. Because iNOS did not colocalize with the red fluorescent label (Fig. 13), we did not attempt a three-label study of OX42, iNOS, and the red fluorescent dye.

Fluorescent red staining significantly increased after IPC and diazoxide (Figs. 6, 7). The pattern of increased red fluorescence was, in both instances, essentially parallel to that of eNOS. Increased red fluorescent labeling after IPC and diazoxide was almost completely blunted by 5-HD (Figs. 8, 9).

## DISCUSSION

The main findings of our study were as follows: (1) IPC was attenuated by blocking the opening of mKATP channels; conversely, IPC was stimulated by opening the channels. The effects of opening the channels were completely reversed by the specific mKATP channel blocker 5-HD. (2) PKC, ROS originating in mitochondria, and NO were downstream transduction elements from mKATP channels in this neuroprotection. (3) Endothelial NOS appears to be

the NOS subtype involved in IPC, because blockade of i- and nNOS did not alter mimicking of IPC by diazoxide. (4) Mitochondrial ROS colocalizes in specific retinal cells with e- and nNOS subtypes after the opening of mKATP channels.

The findings of the present study extend our earlier observations in which we determined that adenosine A1 and A2a receptor activation was an early triggering event after IPC.<sup>19</sup> Mimicking of IPC by adenosine receptor activation was attenuated by blockade of KATP channels or by inhibition of PKC.<sup>14</sup> Furthermore, our earlier finding of altered protein phosphorylation by IPC accords with the essential role of PKC demonstrated in the present study.<sup>18</sup> Examination of the mechanisms downstream from adenosine, mKATP channels, and PKC appears the most promising avenue to uncovering specific endogenously based strategies to treat or prevent damage from retinal ischemia.

The lack of molecular characterization of mKATP channels has led to controversy about their physiological function, and some have even questioned their existence.<sup>24</sup> However, results of five types of studies (recently reviewed by O'Rourke<sup>25</sup>) support the existence and functional role of mKATP. In brief, these include: (1) Direct detection of single-channel activity in the inner mitochondrial membrane as well as channels sensitive to K<sup>+</sup> channel openers and inhibitors in purified inner mitochondrial membrane preparations; (2) K<sup>+</sup> uptake into purified inner mitochondrial preparations; (3) Regulation of mitochondrial swelling by mKATP; (4) Link between mKATP opening and mitochondrial redox state via flavoprotein oxidation; and (5) Opening of the mKATP alters the mitochondrial proton motive force.<sup>25</sup>

Previous experiments suggested existence of the mKATP channel in retina. Kir6.1 components have been found in retinal neurons and in Müller cells in the frog.<sup>26,27</sup> Retinal cells exposed to glutamate were protected by the mKATP channel opener diazoxide.<sup>10</sup> Our data show that opening mKATP with diazoxide mimics IPC protection, whereas IPC or diazoxide's IPC mimicking is blocked by inhibition of mKATP opening with 5-HD, implicating mKATP channels as principal IPC effectors in the retina.

Diazoxide is an antihypertensive agent; however, only a minor decrease in blood pressure was found in our experiments.<sup>6</sup> Thus, systemic changes do not account for the IPC-mimicking by diazoxide. Controversy has developed regarding in vitro and molecular modeling studies that suggest the possibility that diazoxide and 5-HD affect mitochondrial respiration independent of mKATP channels via succinate dehydrogenase (SDH).<sup>28,29</sup> However, a recent study showing that SDH is a component of mKATP as part of a macromolecular signaling complex has lessened this concern.<sup>30</sup> Available data suggest that SDH inhibition is most likely not the underlying mechanism of protection due to K<sup>+</sup> channel openers.<sup>25</sup>

Plausible mechanisms to explain protective effects of K<sup>+</sup> entry via mKATP include: (1) ROS release<sup>31</sup>; (2) activation of NO, PKC, and p38<sup>32</sup>; (3) mitochondrial matrix swelling, decreased nucleotide transport across the voltage-dependent anion channel, and ATP preservation<sup>33, 34</sup>; (4) mitochondrial depolarization and decreased Ca<sup>+2</sup> entry<sup>35-39</sup>; (5) decreased cytochrome *c* and apoptotic Bax and Bad, increased anti-apoptotic Bcl-2.<sup>7,40</sup> Of note, some of the same mechanisms, particularly ROS production, overlap those seen with mitochondrial dysfunction, similar to the paradoxical mechanisms we observed in IPC versus ischemia-reperfusion injury.<sup>18</sup> A paradoxical effect of ROS is notable because they are widely accepted as pathogenic in ischemia, yet evidence is emerging<sup>41</sup> that ROS are part of a pathway to ischemic tolerance. In our study, we have shown that PKC and NO are downstream from the mKATP in the induction of ischemic tolerance. Significant changes in O<sub>2</sub> free radical production specifically in mitochondria, and colocalization with NOS isotypes suggest a role for ROS in the retinal IPC response.

We investigated whether PKC was involved in IPC as a downstream transduction element from the mKATP channel. Chelerythrine ( $IC_{50} = 660 \text{ nM}$ )<sup>23</sup> and Bis1 ( $IC_{50} = 10 \text{ nM}$ ) selectively inhibited PKC, although Davies et al.<sup>42</sup> raised concerns about lack of specificity of Bis1. However, to counter this potential drawback, we followed their suggested approach of testing two structurally unrelated inhibitors to provide greater certainty that we were in fact testing the effect of blocking PKC.<sup>42</sup> PKC phosphorylates a wide variety of proteins and is significant in numerous cellular processes.<sup>43</sup> Rat retina has seven known PKC isoforms:  $\alpha$ ,  $\beta$ ,  $\delta$ ,  $\epsilon$ ,  $\theta$ ,  $\zeta$ , and  $\lambda$ .<sup>44</sup> We have shown that PKC, downstream of adenosine receptors, is involved in IPC in the retina.<sup>14</sup> In the present study, we directly demonstrated that PKC is downstream of the mKATP channel. Further study is necessary to identify the PKC isotypes that are involved, as well as the nature of the downstream proteins that are phosphorylated by activated PKC.

Regarding NO, we found significant increases in e-, i-, and nNOS after both IPC and diazoxide and demonstrated specific cellular localizations (i.e., eNOS in endothelial cells, iNOS in microglia, and nNOS in RGCs). These increases, which were of rapid onset, occurred within the first 24 hours after the IPC stimulus or after IPC-mimicking by diazoxide, and are consistent with the previously demonstrated time window for IPC protection.<sup>13,14</sup> Although nonspecific blockade of NOS by LNNA inhibited IPC and diazoxide mimicking, there was no effect of the specific i- and nNOS blockers 1400W and 7-NI, respectively.<sup>45,46</sup> These data suggest that the NO produced downstream from mKATP channel opening originates from eNOS in retinal endothelial cells. Although the role of NOS in retinal ischemia remains controversial, our results are in line with those in previous reports that blockade of constitutive NOS worsens outcome after ischemia and that upregulated eNOS protects blood-retinal barrier in the L-arginine-treated ischemic rat retina.<sup>47-49</sup>

We showed increased ROS after IPC and diazoxide, as reflected by staining of a red fluorescent dye (MitoTracker; Invitrogen). ROS localization to RGCs and the IPL agrees with findings of our study of enhanced b-wave recovery after ischemia in retinas treated with diazoxide, resulting in protection of the inner retina. Results with the tracer were confirmed by similar results using dihydroethidium, which detects  $O_2$  relatively specifically by two-electron oxidation forming ethidium bromide.  $H_2O_2$ , HOCl, and OONO reaction is minimal. Detection of  $O_2^-$  and  $OH^-$  by the fluorescent label depends on mitochondrial ROS oxidation yielding red fluorescence.<sup>50</sup> Because both HET and the fluorescent dye colocalized with COX IV, it is clear we are measuring mitochondrial ROS. Concerns about cytoplasmic dye quenching are not present because this effect does not occur in fixed tissue.<sup>51-53</sup>

Mitochondrial complex III-generated ROS<sup>54,55</sup> have received the most attention as a potential mechanism of mKATP channel opening cardio- and neuroprotection.<sup>5,56</sup> ROS increase mitochondrial membrane permeability and cytochrome *c* and activate caspases, but paradoxically may trigger a cell stress response leading to cardio- or neuroprotection.<sup>57,58</sup> The retina is unusual in its vulnerability to oxidative light stress; however, some retinal cells, especially RGCs, appear to have as yet unexplained endogenous resistance to ROS.<sup>59</sup> How ROS production is protective has not been completely elucidated, although it is plausible that PKC and other kinases such as p38, as well as NO, are downstream.<sup>56,60,61</sup> The colocalization of ROS and eNOS in endothelial cells suggests an interaction within the vasculature that triggers endogenous neuroprotection. However, ROS were also present after mKATP channel opening in nNOS-containing cells including RGCs or displaced amacrine cells, suggesting that multiple cellular mechanisms are involved in the generation of protective responses by ROS.

In summary, we showed that IPC in the retina requires opening of the mKATP channel and that IPC is effectively mimicked by the mKATP channel opener diazoxide. Both NO, produced by eNOS activation, PKC, and ROS are activated by opening of the mKATP. Further studies

are necessary to determine the specific PKC subtypes involved, as well as the function of ROS in this robust endogenous neuroprotective effect.

## Acknowledgements

Supported by Grant EY10343 from the National Eye Institute (SR), and by a grant from the Illinois Society for the Prevention of Blindness (SR). Digital imaging was performed at the Digital Light Microscopy Facility, University of Chicago Cancer Research Center.

## References

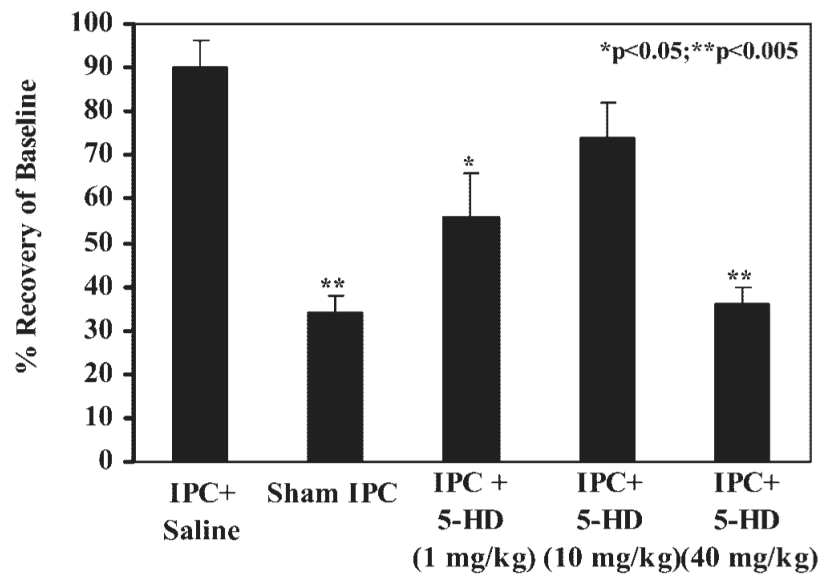
1. Bajgar R, Seetharaman S, Kowaltowski AJ, Garlid KD, Paucek P. Identification and properties of a novel intracellular (mitochondrial) ATP-sensitive potassium channel in brain. *J Biol Chem* 2001;276:33369–33374. [PubMed: 11441006]
2. Lacza Z, Snipes JA, Kis B, Szabo C, Grover G, Busija DW. Investigation of the subunit composition and the pharmacology of the mitochondrial ATP-dependent K<sup>+</sup> channel in the brain. *Brain Res* 2003;994:27–36. [PubMed: 14642445]
3. Sato T, Sasaki N, Seharaseyon J, O'Rourke B, Marban E. Selective pharmacological agents implicate mitochondrial but not sarcolemmal K(ATP) channels in ischemic cardioprotection. *Circulation* 2000;101:2418–2423. [PubMed: 10821820]
4. Domoki F, Perciaccante J, Veltkamp R, Bari F, Busija DW. Mitochondrial potassium channel opener diazoxide preserves neuronal-vascular function after cerebral ischemia in newborn pigs. *Stroke* 1999;30:2713–2718. [PubMed: 10583002]
5. Liu D, Slevin JR, Lu C, et al. Involvement of mitochondrial K<sup>+</sup> release and cellular efflux in ischemic and apoptotic neuronal death. *J Neurochem* 2003;86:966–979. [PubMed: 12887694]
6. Shimizu K, Lacza Z, Rajapakse N, Horiguchi T, Snipes J, Busija DW. MitoK(ATP) opener, diazoxide, reduces neuronal damage after middle cerebral artery occlusion in the rat. *Am J Physiol* 2002;283:H1005–H1011.
7. Liu D, Lu C, Wan R, Auyeung WW, Mattson MP. Activation of mitochondrial ATP-dependent potassium channels protects neurons against ischemia-induced death by a mechanism involving suppression of Bax translocation and cytochrome c release. *J Cereb Blood Flow Metab* 2002;22:431–443. [PubMed: 11919514]
8. Horiguchi T, Kis B, Rajapakse N, Shimizu K, Busija DW. Opening of mitochondrial ATP-sensitive potassium channels is a trigger of 3-nitropropionic acid-induced tolerance to transient focal cerebral ischemia in rats. *Stroke* 2003;34:1015–1020. [PubMed: 12649508]
9. Teshima Y, Akao M, Li RA, et al. Mitochondrial ATP-sensitive potassium channel activation protects cerebellar granule neurons from apoptosis induced by oxidative stress. *Stroke* 2003;34:1796–1802. [PubMed: 12791941]
10. Yamauchi T, Kashii S, Yasuyoshi H, Zhang S, Honda Y, Akaike A. Mitochondrial ATP-sensitive potassium channel: a novel site for neuroprotection. *Invest Ophthalmol Vis Sci* 2003;44:2750–2756. [PubMed: 12766083]
11. Perez-Pinzon MA. Neuroprotective effects of ischemic preconditioning in brain mitochondria following cerebral ischemia. *J Bioeng Biomemb* 2004;36:323–327.
12. Eliseev RA, VanWinkle B, Rosier RN, Gunter TE. Diazoxide-mediated preconditioning against apoptosis involves activation of cAMP-response element binding protein (CREB) and NFκB. *J Biol Chem* 2004;279:46748–46754. [PubMed: 15326191]
13. Roth S, Li B, Rosenbaum PS, et al. Preconditioning provides complete protection against retinal ischemic injury in rats. *Invest Ophthalmol Vis Sci* 1998;39:775–785.
14. Li B, Yang C, Rosenbaum DM, Roth S. Signal transduction mechanisms involved in ischemic preconditioning in the rat retina in vivo. *Exp Eye Res* 2000;70:755–765. [PubMed: 10843780]
15. Nonaka A, Kiryu J, Tsujikawa A, et al. Inhibitory effect of ischemic preconditioning on leukocyte participation in retinal ischemiareperfusion injury. *Invest Ophthalmol Vis Sci* 2001;42:2380–2385. [PubMed: 11527953]



16. Sakamoto K, Kuwagata M, Nakahara T, Ishii K. Late preconditioning in rat retina: involvement of adenosine and ATP-sensitive K<sup>+</sup> channel. *Eur J Pharmacol* 2001;418:89–93. [PubMed: 11334869]
17. Roth S, Shaikh AR, Hennelly MM, Li Q, Bindokas V, Graham CE. Mitogen-activated protein kinases and retinal ischemia. *Invest Ophthalmol Vis Sci* 2003;44:5383–5395. [PubMed: 14638742]
18. Zhang C, Rosenbaum DM, Shaikh AR, et al. Ischemic preconditioning attenuates apoptosis following retinal ischemia in rats. *Invest Ophthalmol Vis Sci* 2002;43:3059–3066. [PubMed: 12202530]
19. Li B, Roth S. Retinal ischemic preconditioning in the rat: requirement for adenosine and repetitive induction. *Invest Ophthalmol Vis Sci* 1999;40:1200–1216. [PubMed: 10235554]
20. Lin J, Roth S. Retinal hypoperfusion after ischemia in rats: attenuation by ischemic preconditioning. *Invest Ophthalmol Vis Sci* 1999;40:2925–2931. [PubMed: 10549654]
21. Junk AK, Mammis A, Savitz SI, et al. Erythropoietin administration protects retinal neurons from acute ischemia-reperfusion injury. *Proc Natl Acad Sci USA* 2002;99:10659–10664. [PubMed: 12130665]
22. Toullec D, Pianetti P, Coste H, et al. The bisindolylmaleimide GF 109203X is a potent and selective inhibitor of protein kinase C. *J Biol Chem* 1991;266:15771–15781. [PubMed: 1874734]
23. Herbert JM, Augereau JM, Gleye J, Maffrand JP. Chelerythrine is a potent and specific inhibitor of protein kinase C. *Biochem Biophys Res Commun* 1990;172:993–999. [PubMed: 2244923]
24. Inoue I, Nagase H, Kishi K, Higuti T. ATP-sensitive K<sup>+</sup> channel in the mitochondrial inner membrane. *Nature* 1991;352:244–247. [PubMed: 1857420]
25. O'Rourke B. Evidence for mitochondrial K<sup>+</sup> channels and their role in cardioprotection. *Circ Res* 2004;94:420–432. [PubMed: 15001541]
26. Skatchkov SN, Thomzig A, Eaton MJ, et al. Kir subfamily in frog retina: specific spatial distribution of Kir 6.1 in glial (Muller) cells. *Neuroreport* 2001;12:1437–1441. [PubMed: 11388425]
27. Skatchkov SN, Rojas L, Eaton MJ, et al. Functional expression of Kir 6.1/SUR1-K(ATP) channels in frog retinal Muller glial cells. *Glia* 2002;38:256–267. [PubMed: 11968063]
28. Hanley PJ, Mickel M, Loffler M, Brandt U, Daut J. K(ATP) channel-independent targets of diazoxide and 5-hydroxydecanoate in the heart [see comment]. *J Physiol* 2002;542:735–741. [PubMed: 12154175]
29. Hanley PJ, Gopalan KV, Lareau RA, Srivastava DK, von Meltzer M, Daut J. Beta-oxidation of 5-hydroxydecanoate, a putative blocker of mitochondrial ATP-sensitive potassium channels. *J Physiol* 2003;547:387–393. [PubMed: 12562916]
30. Ardehali H, Chen Z, Ko Y, Mejia-Alvarez R, Marban E. Multiprotein complex containing succinate dehydrogenase confers mitochondrial ATP-sensitive K<sup>+</sup> channel activity. *Proc Natl Acad Sci USA* 2004;101:11880–11885. [PubMed: 15284438]
31. Oldenburg O, Cohen MV, Downey JM. Mitochondrial K(ATP) channels in preconditioning. *J Mol Cell Cardiol* 2003;35:569–575. [PubMed: 12788373]
32. Cohen MV, Baines CP, Downey JM. Ischemic preconditioning: from adenosine receptor of KATP channel. *Ann Rev Physiol* 2000;62:79–109. [PubMed: 10845085]
33. Dos Santos P, Kowaltowski AJ, Laclau MN, et al. Mechanisms by which opening the mitochondrial ATP-sensitive K(+) channel protects the ischemic heart. *Am J Physiol* 2002;283:H284–H295.
34. Miura T, Liu Y, Kita H, Ogawa T, Shimamoto K. Roles of mitochondrial ATP-sensitive K channels and PKC in anti-infarct tolerance afforded by adenosine A1 receptor activation. *J Am Coll Cardiol* 2000;35:238–245. [PubMed: 10636286]
35. Zhan RZ, Fujihara H, Baba H, Yamakura T, Shimoji K. Ischemic preconditioning is capable of inducing mitochondrial tolerance in the rat brain. *Anesthesiology* 2002;97:896–901. [PubMed: 12357156]
36. Murata M, Akao M, O'Rourke B, Marban E. Mitochondrial ATP-sensitive potassium channels attenuate matrix Ca(2+) overload during simulated ischemia and reperfusion: possible mechanism of cardioprotection. *Circ Res* 2001;89:891–898. [PubMed: 11701616]
37. Wang L, Cherednichenko G, Hernandez L, et al. Preconditioning limits mitochondrial Ca(2+) during ischemia in rat hearts: role of K(ATP) channels. *Am J Physiol* 2001;280:H2321–H2328.

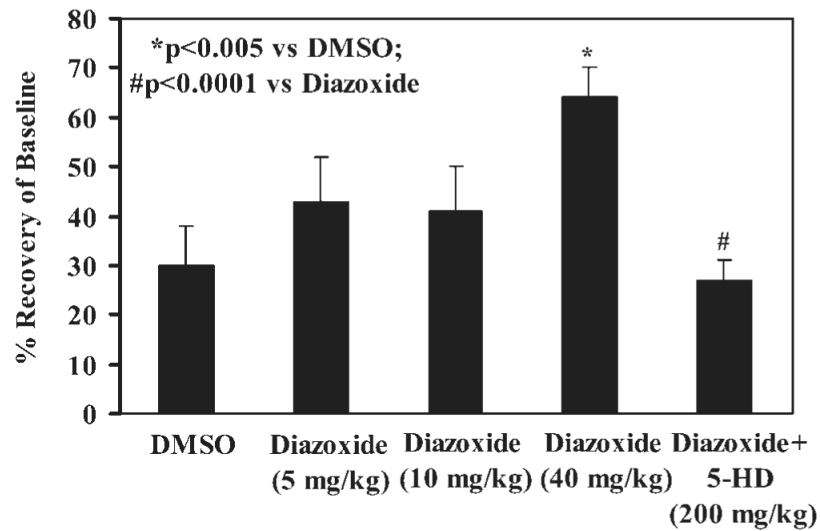
38. Kobayashi T, Kuroda S, Tada M, Houkin K, Iwasaki Y, Abe H. Calcium-induced mitochondrial swelling and cytochrome c release in the brain: its biochemical characteristics and implication in ischemic neuronal injury. *Brain Res* 2003;960:62–70. [PubMed: 12505658]
39. Piriou V, Chiari P, Gateau-Roesch O, et al. Desflurane-induced preconditioning alters calcium-induced mitochondrial permeability transition. *Anesthesiology* 2004;100:581–588. [PubMed: 15108972]
40. Murphy E. Primary and secondary signaling pathways in early preconditioning that converge on the mitochondria to produce cardioprotection. *Circ Res* 2004;94:7–16. [PubMed: 14715531]
41. Mayr M, Metzler B, Chung YL, et al. Ischemic preconditioning exaggerates cardiac damage in PKC-delta null mice. *Am J Physiol* 2004;287:H946–H956.
42. Davies SP, Reddy H, Caivano M, Cohen PC. Specificity and mechanism of action of some commonly used protein kinase inhibitors. *Biochem J* 2000;351:95–105. [PubMed: 10998351]
43. Way KJ, Chou E, King GL. Identification of PKC-isoform-specific biological actions using pharmacological approaches. *Trends Pharmacol Sci* 2000;21:181–187. [PubMed: 10785652]
44. Wood JP, McCord RJ, Osborne NN. Retinal protein kinase C (Review). *Neurochem Int* 1997;30:119–136. [PubMed: 9017660]
45. Hashiguchi A, Yano S, Morioka M, et al. Up-regulation of endothelial nitric oxide synthase via phosphatidylinositol 3-kinase pathway contributes to ischemic tolerance in the CA1 subfield of gerbil hippocampus. *J Cereb Blood Flow Metab* 2004;24:271–279. [PubMed: 15091107]
46. Hardy P, Lamireau D, Hou X, et al. Major role for neuronal NO synthase in curtailing choroidal blood flow autoregulation in newborn pig. *J Appl Physiol* 2001;91:1655–1662. [PubMed: 11568147]
47. Ju WK, Gwon JS, Kim KY, Oh SJ, Kim SY, Chun MH. Up-regulated eNOS protects blood-retinal barrier in the L-arginine treated ischemic rat retina. *Neuroreport* 2001;12:2405–2409. [PubMed: 11496119]
48. Cheon EW, Park CH, Kang SS, et al. Change in endothelial nitric oxide synthase in the rat retina following transient ischemia. *Neuroreport* 2003;14:329–333. [PubMed: 12634478]
49. Hangai M, Miyamoto K, Hiroi K, et al. Roles of constitutive nitric oxide synthase in postischemic rat retina. *Invest Ophthalmol Vis Sci* 1999;40:450–458. [PubMed: 9950605]
50. Kim DY, Won SJ, Gwag BY. Analysis of mitochondrial free radical generation in animal models of neuronal disease. *Free Rad Biol Med* 2002;33:715–723. [PubMed: 12208358]
51. Buckman JF, Hernandez H, Kress GJ, Votyakova TV, Pal S, Reynolds IJ. MitoTracker labeling in primary neuronal and astrocytic cultures: influence of mitochondrial membrane potential and oxidants. *J Neurosci Methods* 2001;104:165–176. [PubMed: 11164242]
52. Pendergrass W, Wolf N, Poot M. Efficacy of MitoTracker Green and CMXRosamine to measure changes in mitochondrial membrane potentials in living cells and tissues. *Cytometry* 2004;61A:162–169. [PubMed: 15382028]
53. Poot M, Zhang Y-Z, Kramer JA, et al. Analysis of mitochondrial morphology and function with novel fixable fluorescent stains. *J Histochem Cytochem* 1996;44:1363–1372. [PubMed: 8985128]
54. Chen Q, Vazquez EJ, Moghaddas S, Hoppel CL, Lesnefsky EJ. Production of reactive oxygen species by mitochondria: central role of complex III. *J Biol Chem* 2003;278:36027–36031. [PubMed: 12840017]
55. Chandel NS, McClintock DS, Feliciano CE, et al. Reactive oxygen species generated at mitochondrial complex III stabilize hypoxia-inducible factor-1alpha during hypoxia: a mechanism of O<sub>2</sub> sensing. *J Biol Chem* 2000;275:25130–25138. [PubMed: 10833514]
56. Lebuffe G, Schumacker PT, Shao ZH, Anderson T, Iwase H, Vanden Hoek TL. ROS and NO trigger early preconditioning: relationship to mitochondrial KATP channel. *Am J Physiol* 2003;284:H299–H308.
57. Gross GJ, Peart JN. KATP channels and myocardial preconditioning: an update. *Am J Physiol* 2003;285:H921–H930.
58. Mattson MP, Kroemer G. Mitochondria in cell death: novel targets for neuroprotection and cardioprotection. *Trends Mol Med* 2003;9:196–205. [PubMed: 12763524]
59. Kortuem K, Geiger LK, Levin LA. Differential susceptibility of retinal ganglion cells to reactive oxygen species. *Invest Ophthalmol Vis Sci* 2000;41:3176–3182. [PubMed: 10967081]

60. Lin YF, Raab-Graham K, Jan YN, Jan LY. NO stimulation of ATP-sensitive potassium channels: involvement of Ras/mitogen-activated protein kinase pathway and contribution to neuroprotection. *Proc Natl Acad Sci USA* 2004;101:7799–7804. [PubMed: 15136749]
61. Levrault J, Wase H, Shao Z, H. Vanden Hoek T L, Schumacker P T. Cell death during ischemia: relationship to mitochondrial depolarization and ROS generation. *Am J Physiol* 2003;285:H549-H558.



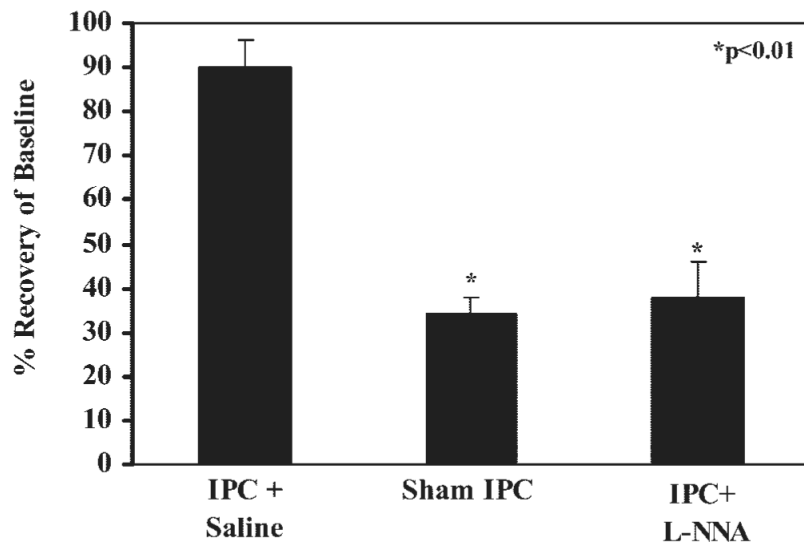
**FIGURE 1.**

5-HD blocked the neuroprotective effects of IPC in a dose-dependent manner. IPC (8 minutes of increased intraocular pressure) was performed 24 hours before 45 minutes of ischemia. The b-wave was measured at baseline and at 7 days after ischemia; results shown at 7 days in the ischemic eye were normalized to baseline and for day-to-day variation in the control, nonischemic eye. The *leftmost* bar shows that IPC ( $n = 10$  rats) resulted in nearly complete recovery of the ERG b-wave (y-axis) relative to preischemic baseline. Data are shown as the mean  $\pm$  SEM. The ERG b-wave recovery was significantly reduced when 5-HD 1 mg/kg ( $P < 0.03$ ,  $n = 4$  rats) and 40 mg/kg ( $P < 0.005$ ,  $n = 4$  rats) was injected before IPC. The blunting of recovery after IPC by 5-HD approaches that of sham IPC (second bar from *left*).



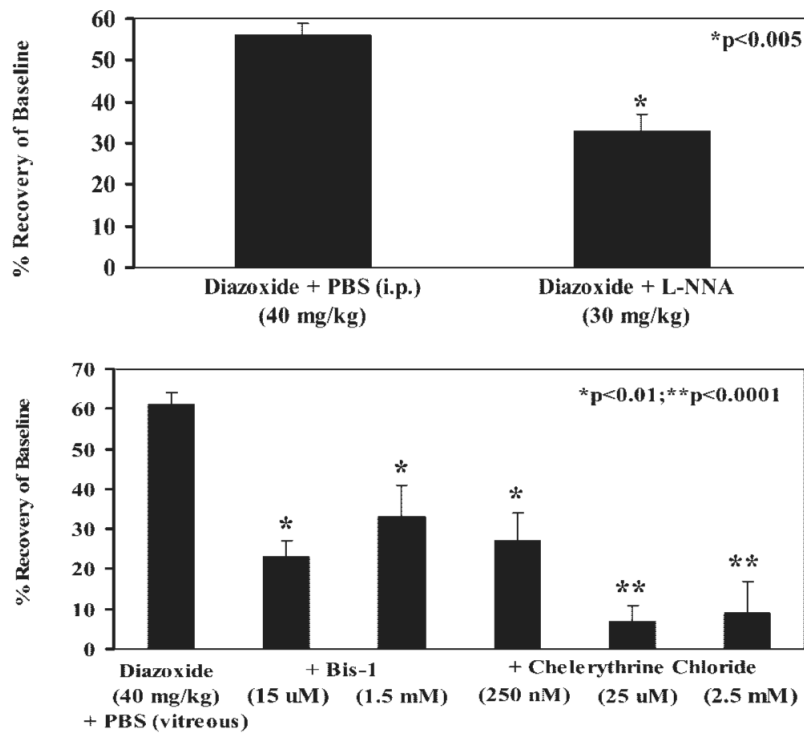
**FIGURE 2.**

The mKATP agonist, diazoxide, mimicked the neuroprotective effects of IPC in a dose-dependent manner. Diazoxide was injected IP 24 hours before 45 minutes of ischemia and compared with injection of DMSO vehicle (*leftmost* bar). See Figure 1 for a description of the method. The significant IPC-mimicking by diazoxide ( $P < 0.004$ ) 40 mg/kg was inhibited by 5-HD (200 mg/kg,  $P < 0.0003$  vs. diazoxide).  $n = 10$  rats in the diazoxide 40-mg/kg group, and five to seven rats in the others.

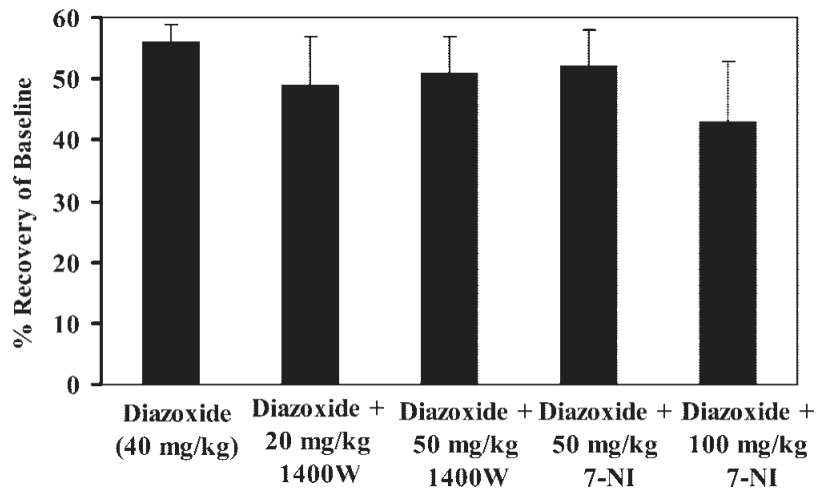


**FIGURE 3.**

The nonspecific NOS inhibitor L-NNA 30 mg/kg significantly attenuated the neuroprotective effect of IPC ( $P < 0.01$ ). L-NNA was injected IP before IPC, which was followed 24 hours later by 45 minutes of ischemia. See Figure 1 for a description of the method. Sham IPC ( $n = 13$  rats) shows no significant difference versus L-NNA+IPC ( $n = 5$ ).

**FIGURE 4.**

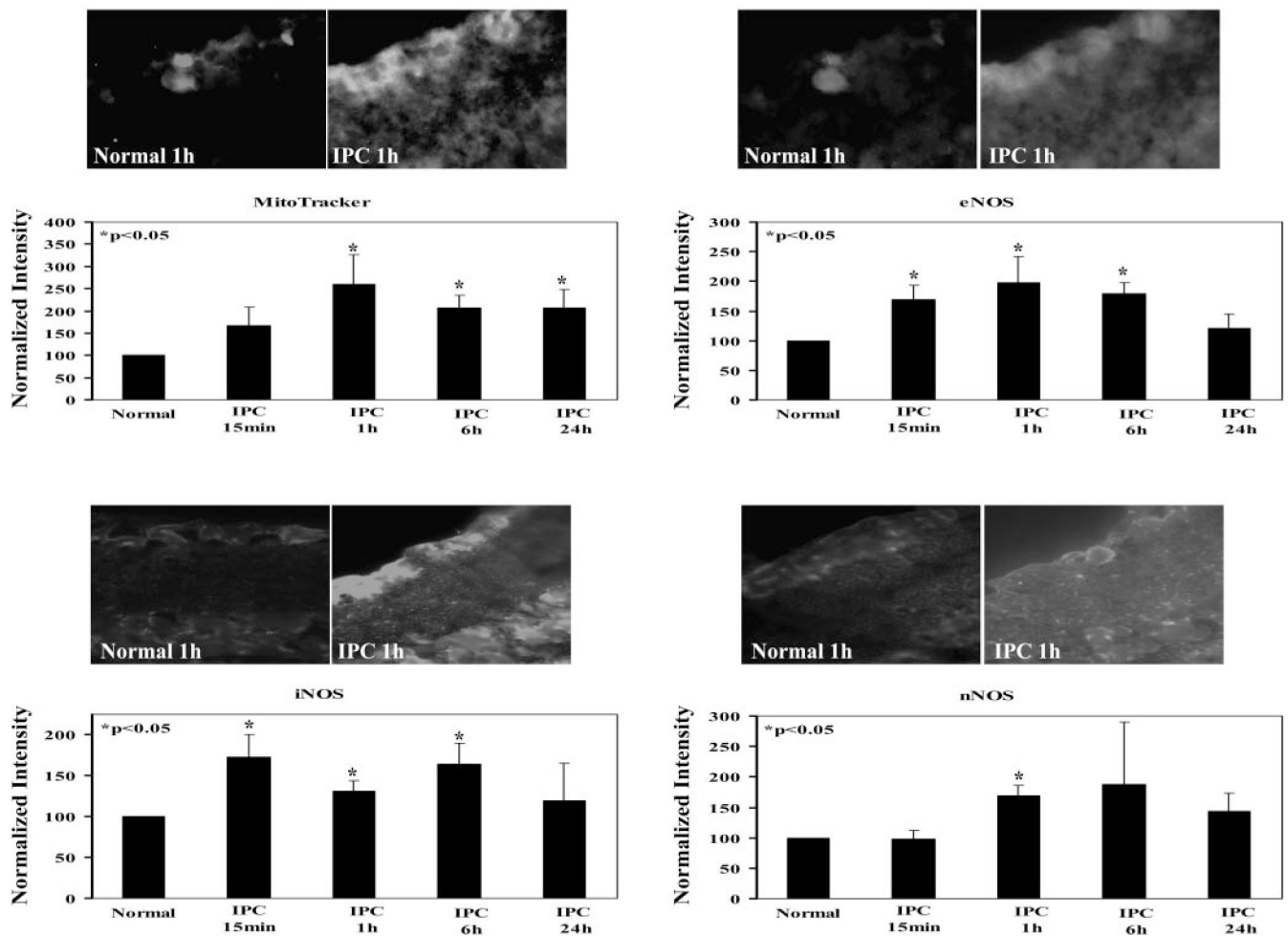
L-NNA 30 mg/kg significantly blocked (*top*,  $P < 0.002$ ,  $n = 5$  rats) the IPC-mimicking of diazoxide (40 mg/kg,  $n = 8$  rats). In addition, the PKC inhibitors Bis1 or chelerythrine (*bottom*), injected into the vitreous at the time of IP injection of diazoxide, significantly diminished IPC mimicking (compared with diazoxide 40 mg/kg+PBS vehicle in vitreous,  $n = 9$ ): Bis1 15  $\mu$ M ( $P < 0.009$ ,  $n = 3$  rats) and 1.5 mM ( $P < 0.008$ ,  $n = 4$  rats), and chelerythrine 250 nM ( $P < 0.01$ ,  $n = 11$  rats), 25  $\mu$ M ( $P < 0.0001$ ,  $n = 6$  rats), and 2.5 mM ( $P < 0.0001$ ,  $n = 6$  rats). See Figure 1 for a description of the method.



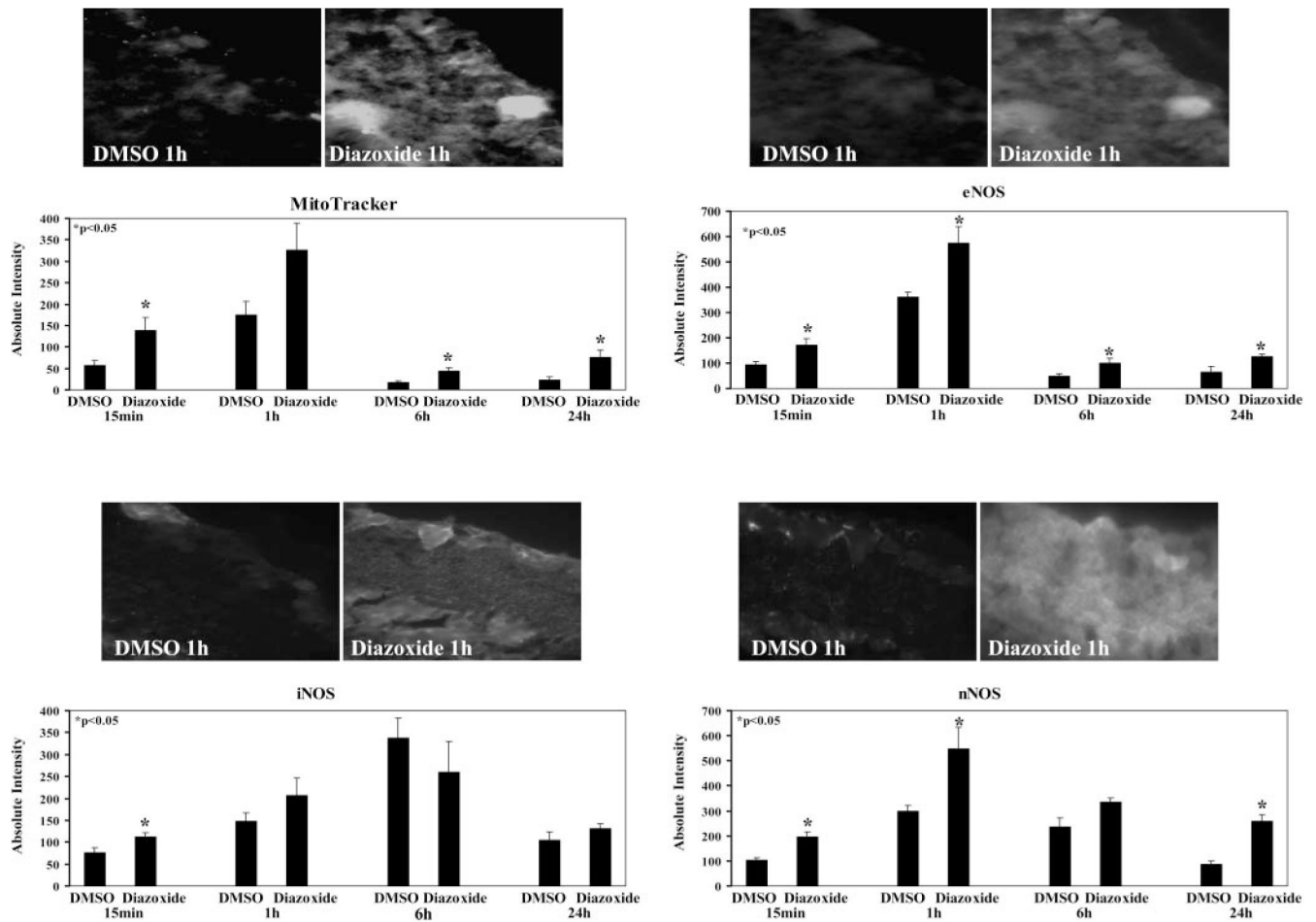
**FIGURE 5.**

The IPC-mimicking effect of diazoxide was not affected by either the specific iNOS inhibitor 1400W or the specific nNOS antagonist 7-NI ( $n = 4 - 8$  rats per group). Both inhibitors were injected IP before diazoxide, and ischemia was induced 24 hours later. See Figure 1 for a description of the method.

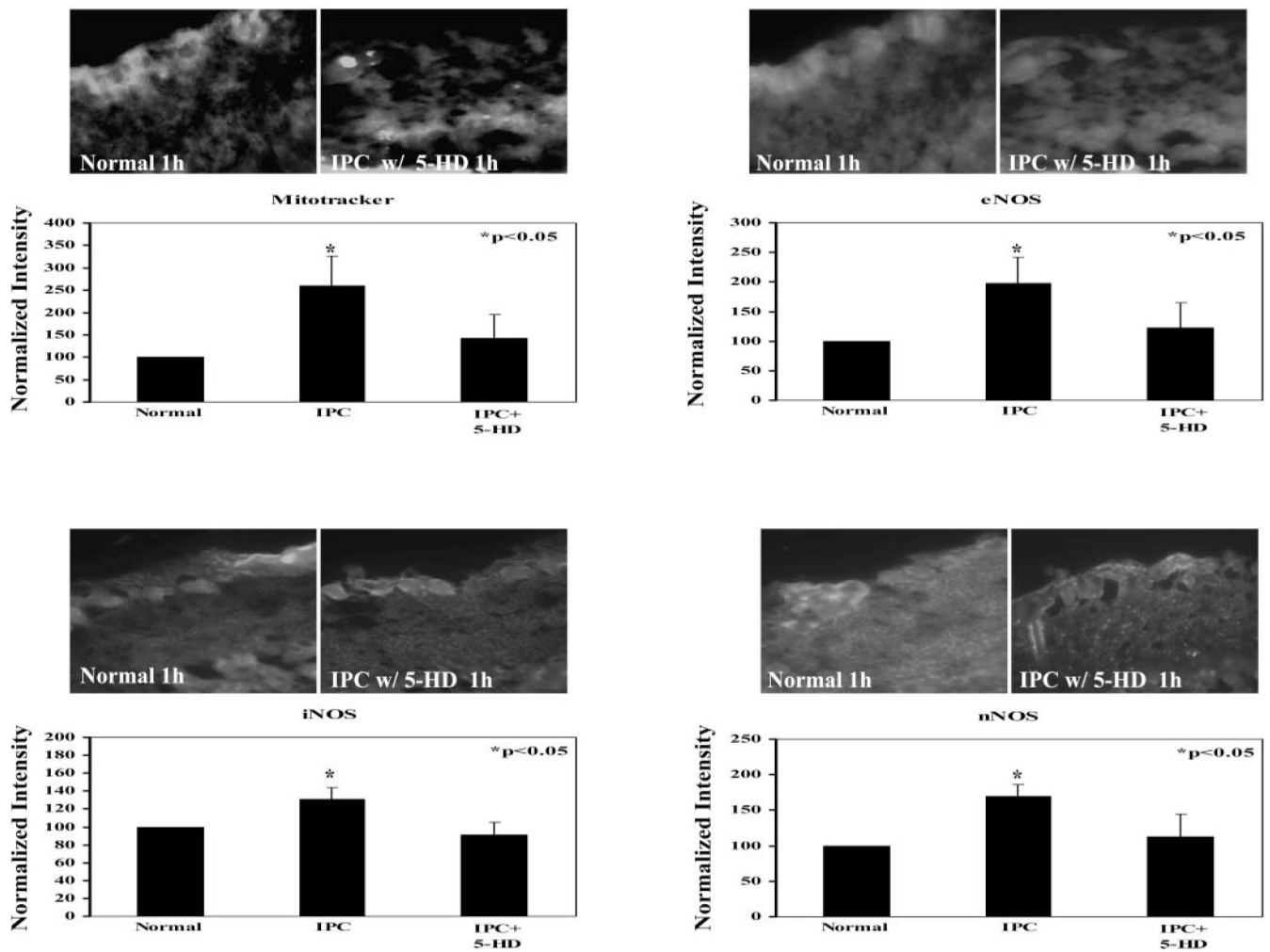


**FIGURE 6.**

IPC increased both ROS generation and NOS subtype expression in the retina. Each time point after IPC represents the normalized intensity in the inner retina relative to the matched normal (sham IPC) paired eyes. The quantitation of the fluorescence-labeled (MitoTracker; Invitrogen) immunohistochemical retinal sections ( $n = 3-6$  rats per group) shows that ROS generation was significantly ( $P < 0.05$ ) increased at 1, 6, and 24 hours after IPC. The expression of both eNOS and iNOS was significantly increased at 15 minutes and 1 and 6 hours after IPC. nNOS expression was significantly increased at 1 hour after IPC. Representative images for the fluorescent labeling (MitoTracker; Invitrogen) and each NOS subtype are shown above each graph for a normal and IPC retinal section 1 hour after IPC.

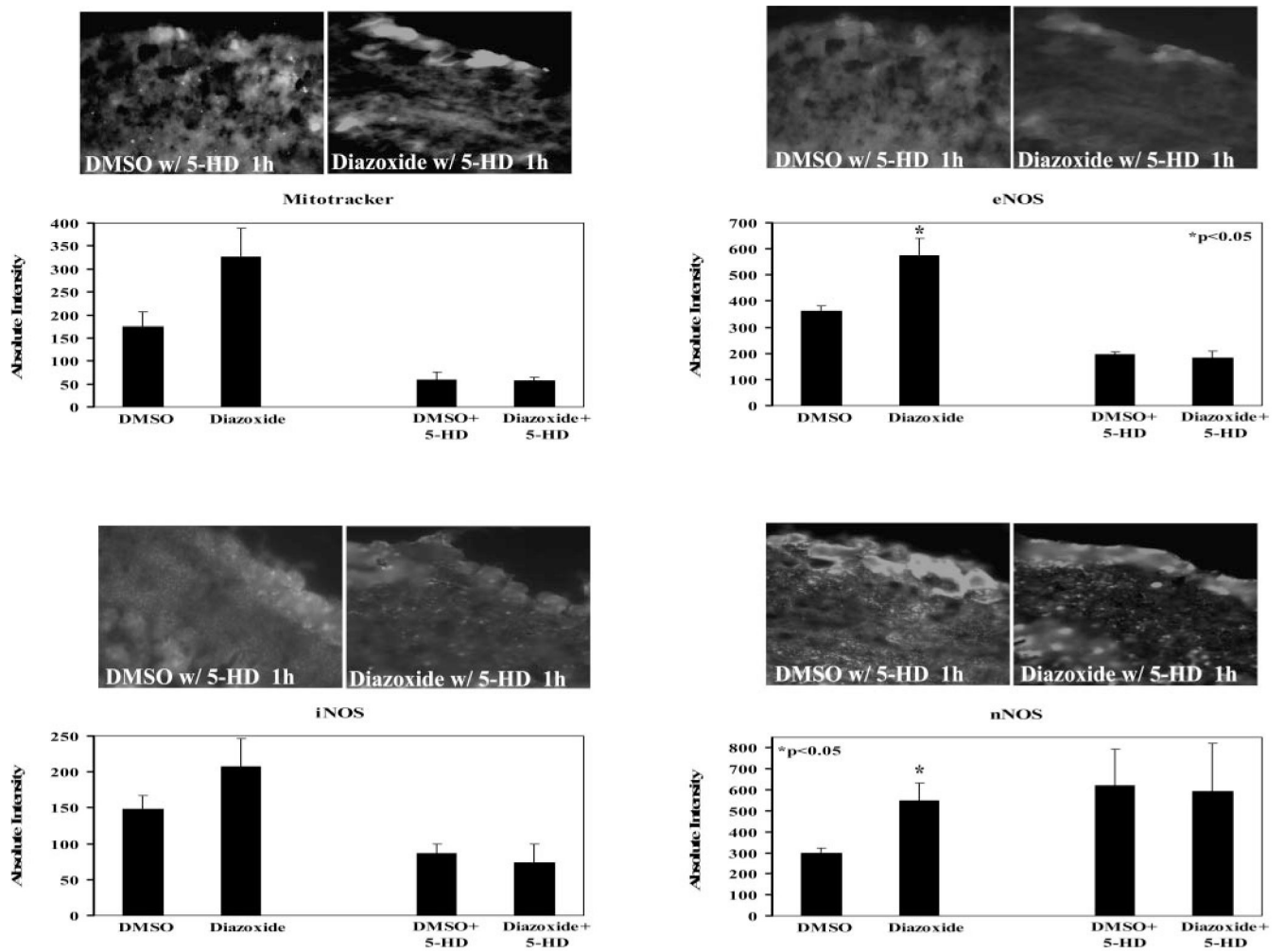
**FIGURE 7.**

Diazoxide (40 mg/kg) increased both ROS generation and NOS subtype expression in the retina. Each pair of bars represents absolute intensity in the inner retina for the matched time point after diazoxide or DMSO-vehicle injection. See Figure 6 for a description of the method. Quantitation of the fluorescence-labeled immunohistochemical retinal sections ( $n = 4 - 6$  rats per group) showed that ROS generation was significantly ( $P < 0.05$ ) increased at 15 minutes and 6 and 24 hours after diazoxide stimulation. The trend for increase at 1 hour was not significant. The expression of eNOS is significantly increased at all four time points after diazoxide. iNOS is significantly increased only at 15 minutes after diazoxide. nNOS expression was significantly increased at 15 minutes and 1 and 24 hours after diazoxide. Representative images of the fluorescent labeling and for each NOS subtype are shown above each graph for vehicle control and diazoxide retinal section at 1 hour.



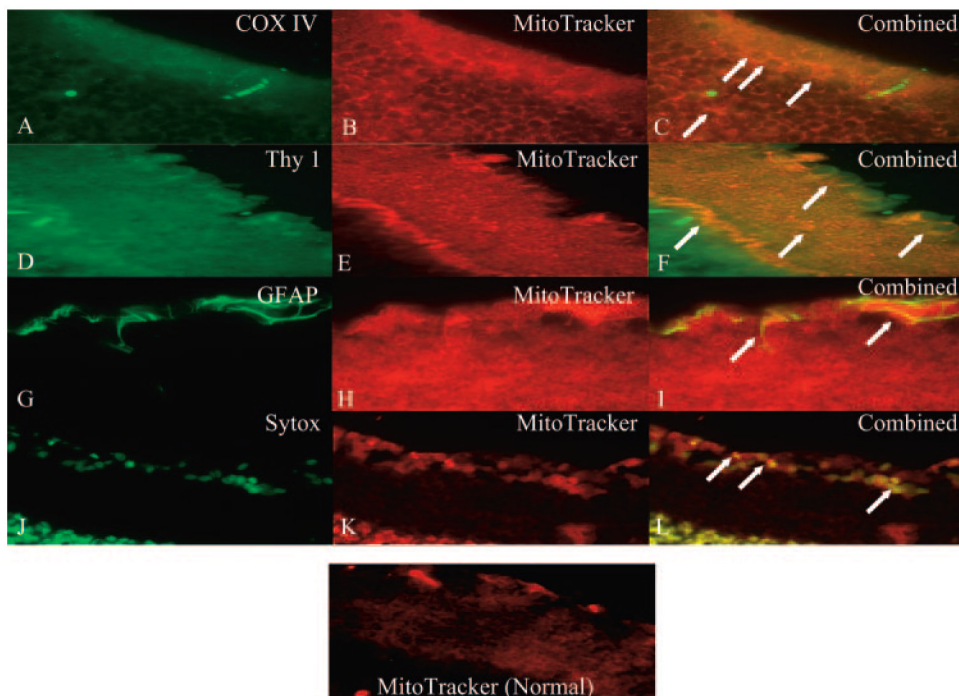
**FIGURE 8.**

The mKATP inhibitor 5-HD blocked IPC-induced ROS generation and NOS subtype expression ( $n = 3-6$  rats). Representative images of the fluorescent labeling and each NOS subtype are shown above each graph for a normal and IPC retinal section 1 hour after IPC with preceding 5-HD application. The fluorescent images were taken at different exposure times than those used for Figure 6.



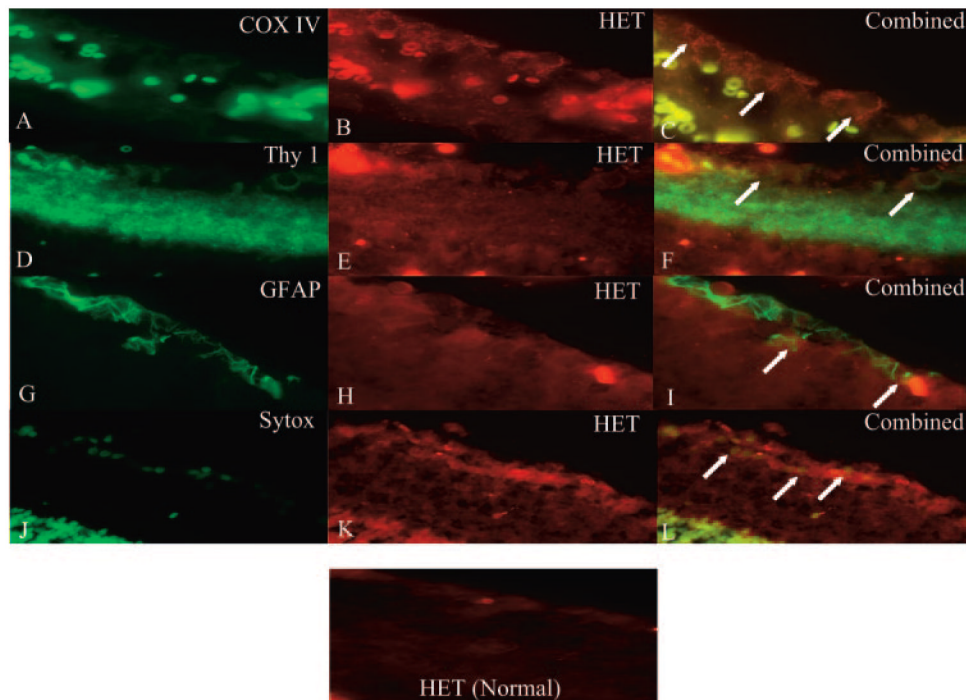
**FIGURE 9.**

The mKATP inhibitor 5-HD blocks the diazoxide-induced ROS generation and NOS subtype expression ( $n = 4 - 6$  rats). Representative images of the fluorescent labeling and each NOS subtype are shown above each graph for a normal and IPC retinal section 1 hour after diazoxide and 5-HD application. The fluorescent images were taken at different exposure times than those used for Figure 7.



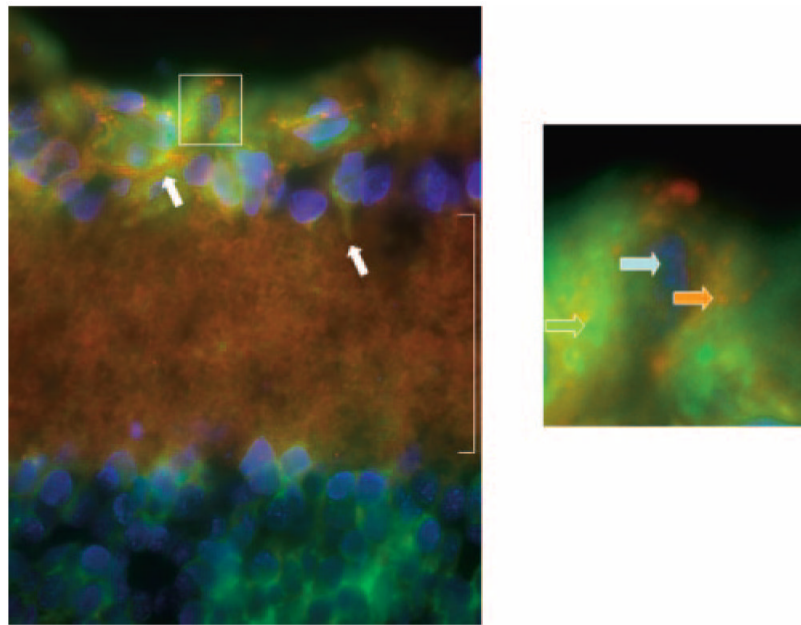
**FIGURE 10.**

Images of 10- $\mu$ m retinal cryosections. The mitochondrial inner membrane marker (COX IV; **A**), an RGC marker (Thy-1; **D**), a glial cell marker (GFAP; **G**) and a nuclear marker (**J**; Sytox; Invitrogen) are depicted in the *leftmost* columns. The red fluorescent label (MitoTracker; Invitrogen) shows the generation of ROS in ischemic retinal sections (**B**, **E**, **H**, **K**). Combined images, in which *yellow* or *orange* indicate colocalization (*white arrows*). ROS localization in the mitochondria is confirmed by colocalization of red fluorescence and COX IV and intracellular localization to RGCs and Müller cells by Thy-1, GFAP, and nucleic acid staining (**C**, **F**, **I**, **J**). *Bottom*: nonischemic negative control section with minimal positive staining. Magnification, x63.



**FIGURE 11.**

Shown are 63x images of 10- $\mu$ m retinal cryosections. The mitochondrial marker (COX IV; **A**), an RGC marker (Thy-1; **D**), a glial cell marker (GFAP; **G**) and the nuclear marker (Sytox; **J**) are depicted in the *leftmost* columns. Dihydroethidium (HET) shows the generation of ROS in ischemic retinal sections (**B, E, H, K**) in the *middle* columns. The combined images showing colocalization (yellow or orange; white arrows) are shown in the *rightmost* columns (**C, F, I, J**). A nonischemic negative control section with minimal positive staining appears at the *bottom middle* for comparison. The results with HET confirm those with the red fluorescent label (MitoTracker; Invitrogen) in Figure 10. Magnification, x63.

**FIGURE 12.**

Red fluorescence (MitoTracker; Invitrogen) colocalized with COX IV (*green*) in the mitochondria of RGCs (*right, orange arrow*) and in their axonal projections (*left, white arrows*). Note the punctate staining of the mitochondria. Also note that not all mitochondria stained for both markers (*right, green arrow*). The IPL (*left, brackets*) stained intensely for both red fluorescence and COX IV. DAPI *blue* stained the cell nuclei (*right, blue arrow*). *Left*: 63x fluorescent image; *right*: the magnified image of an RGC in the left image's boxed area.

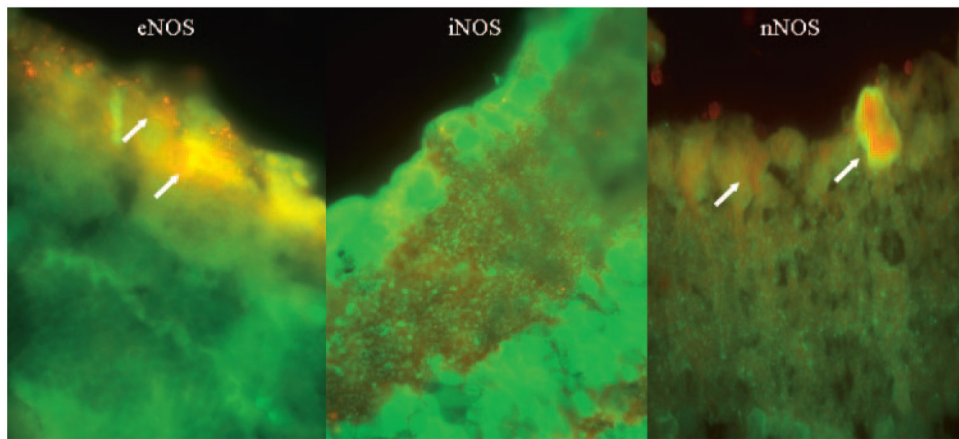


**FIGURE 13.**

Double-labeled 10- $\mu$ m retinal cryosections, the colocalization of red fluorescent dye (Mito-Tracker; Invitrogen) and eNOS (*left, arrows*) and nNOS (*right, arrows*) is evident, whereas iNOS did not colocalize with the red label (*middle*). Magnification x63.



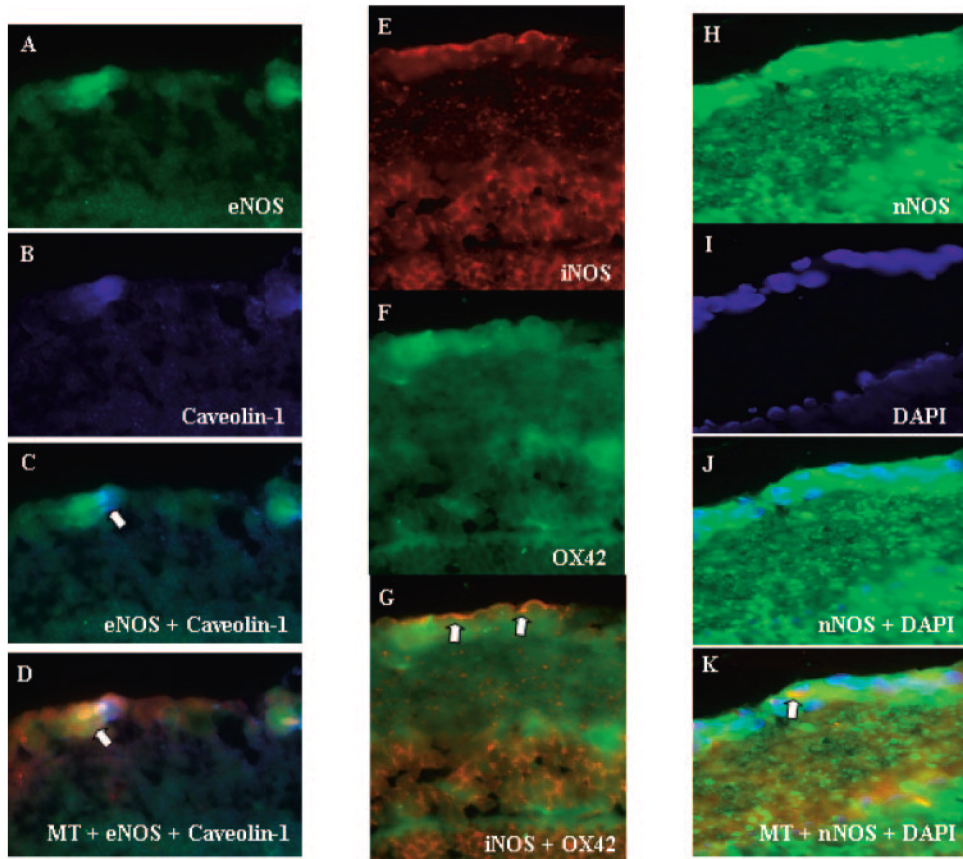


**FIGURE 14.**

In 63x double-labeled 10- $\mu$ m retinal cryosections, images (A—D) show the single immunohisto-chemical staining of eNOS (A) and the endothelial cell marker caveolin-1 (B). There was colocalization of eNOS and caveolin-1 (C, *arrow*) and, in a triple-labeled section, of red fluorescent dye (MitoTracker; Invitrogen), eNOS, and caveolin-1 (D, *arrow*). The expression of iNOS (E) and the microglial marker OX42 (F) show colocalization (G, *arrows*). The nNOS expression in RGCs is seen in (H), and DAPI nuclear staining in (I). The combined image of nNOS and DAPI demonstrating colocalization in RGCs is shown in (J). A triple-labeled section (K), shows the colocalization of nNOS, DAPI, and red fluorescent label in RGCs (*arrow*).